

# Second Branchial Arch Lineages of the Middle Ear of Wild-Type and *Hoxa2* Mutant Mice

Stephen O’Gorman\*

**Our current understanding of the evolution of the mammalian middle ear was first suggested by embryological studies from the 19th century. Here, site-specific recombinase-mediated lineage tracing was used to define the second branchial arch contribution to the middle ear of wild-type and *Hoxa2* mutant embryos. The processus brevis of the malleus was found to arise from second arch tissues, making it the likely homologue of the retroarticular process of nonmammalian tetrapods. The second arch also formed a portion of the otic capsule. In light of avian lineage studies, second arch cells were probably incorporated into the otic capsule before avian and mammalian lineages diverged. In *Hoxa2* mutant embryos, middle ear skeletal duplications occurred at sites where first and second arch elements are normally apposed. The dorsoventral positions at which second arch skeletal elements formed and the early migration of second arch neural crest cells were not altered by the absence of *Hoxa2* function. *Developmental Dynamics* 234: 124–131, 2005. © 2005 Wiley-Liss, Inc.**

**Key words:** middle ear; branchial arm; Hoxb1; Hoxa2; craniofacial development

Received 3 February 2005; Revised 21 February 2005; Accepted 21 February 2005

## INTRODUCTION

The evolution of the mammalian middle ear from skeletal elements that formed the jaw joint of ancestral forms has been a topic of investigation and speculation for nearly 200 years (Strickland and Anson, 1962; Allin, 1975). The middle ears of nonmammalian tetrapods contain a single ossicle, homologous to the mammalian stapes, that conducts sound from the tympanic membrane to the oval window of the inner ear. A similar condition was present in mammalian precursors, but two additional ossicles, the malleus and incus, were incorporated during the evolution of present-day mammals (Romer and Parsons, 1977). Our present understanding of these changes was first suggested by Reichert’s em-

bryological studies (Reichert, 1837). Reichert proposed that the malleus and the incus are derivatives of the articular and quadrate bones that formed the ancestral jaw articulation and that developmentally they arise from the cartilage of the first branchial arch. He also found that the stapes was the principal derivative of the dorsal second arch cartilage, the hyomandibula, in present day tetrapods. In significant respects, these ideas have not been critically evaluated through the generation of mammalian fate maps.

In the absence of such maps, the development of mammalian craniofacial tissues and the craniofacial phenotypes caused by mutations in mammals typically have been interpreted with reference to the detailed fate

maps available for avian embryos (Le Lievre, 1978; Noden, 1978; Kontges and Lumsden, 1996). These maps show that many craniofacial connective tissues and skeletal elements arise from neural crest cells. The mesenchyme of the first branchial arch is generated by neural crest cells arising from the midbrain and the first two segments of the hindbrain, rhombomeres 1 and 2 (r1, r2). The mesenchyme of the second branchial arch, by contrast, is generated by neural crest cells from r4, with minor contributions from r3 and r5 (Lumsden et al., 1991). The crest cell cohorts destined for the first and second arches do not intermingle as they migrate, and remain as coherent, nonoverlapping populations through relatively late

Department of Neurosciences, School of Medicine, Case Western Reserve University, Cleveland, Ohio  
Grant sponsor NIH; Grant number: GM056525

\*Correspondence to: Stephen O’Gorman, Department of Neurosciences, School of Medicine, Case Western Reserve University, 10900 Euclid Avenue, Cleveland, OH 44106. E-mail: ogorman@case.edu

DOI 10.1002/dvdy.20402

Published online 28 April 2005 in Wiley InterScience (www.interscience.wiley.com).

stages of embryogenesis (Kontges and Lumsden, 1996). The use of vital dyes to mark small numbers of crest cells in mouse embryos suggests that mammalian crest cells behave in a similar manner (Serbedzija et al., 1992).

The formation of many craniofacial tissues is influenced by Hox genes. The neural crest populating the first branchial arch does not express any Hox gene, whereas that of the second arch expresses *Hoxa2* over a prolonged period (Couly et al., 1998; Kanzler et al., 1998). Misexpression of *Hoxa2* in first arch crest results in the absence of first arch skeletal elements or the duplication of second arch structures within the first arch domain (Grammatopoulos et al., 2000; Creuzet et al., 2002). By contrast, loss of *Hoxa2* function in the second arch causes the duplication of some first arch elements within the second arch territory (Gendron-Maguire et al., 1993; Rijli et al., 1993). *Hoxa2* thus functions as a selector gene to promote second arch identities in crest-derived mesenchyme. Some alterations observed in *Hoxa2* mutants, such as the absence of the processus brevis of the malleus, the axis of symmetry of the duplication of the squamosal bone, and the malformation of the otic capsule, are not well explained by extrapolations from avian fate maps.

Here, a fate mapping paradigm based on the selective expression of a site-specific recombinase (O'Gorman et al., 1991) has been used to determine how second branchial arch tissues contribute to the mammalian middle ear. Because the r4 neuroepithelium and its derived neural crest transiently express *Hoxb1*, a recombinant allele of *Hoxb1* (*B1<sup>Cre</sup>*) was prepared that expresses Cre recombinase instead of the normal gene product (Zhou et al., manuscript submitted for publication). When this allele was combined with the Cre-conditional *R26R* reporter (Soriano, 1999), virtually all r4-derived crest cells heritably expressed the reporter, allowing the lineage to be followed through later stages. Analysis of the lineage marking in these embryos showed that the malleus was a composite of first and second arch tissues, rather than being entirely derived from the first arch. Surprisingly, second arch neural crest lineage also gave rise to a portion of

the otic capsule that was contiguous with the squamosal bone, a finding that suggests alternative interpretations for the representation of the hyomandibula in modern tetrapods.

## RESULTS

### Labeling of Second Arch Neural Crest by the *B1<sup>Cre</sup>* and *R26R* alleles

Cre expression from the *B1<sup>Cre</sup>* allele in *+ /B1<sup>Cre</sup>, + /R26R* embryos resulted in the activation of  $\beta$ -galactosidase expression from the *R26R*, Cre-conditional marker allele in the r4 neuroepithelium and nearly all neural crest cells that emerged from r4 to populate the second branchial arch (Fig. 1). Second arch tissues not derived from neural crest cells (Le Douarin, 1983), including its mesodermal core, ectoderm, and most neurons of the facial ganglion, were not labeled (Zhou et al., manuscript submitted for publication). By contrast, the neuroepithelium anterior to r4 and tissues of the first branchial arch were negative for marker expression. More posterior regions of the hindbrain and the third branchial arch showed a low level of marker activation, presumably caused by the Cre expression from the *B1<sup>Cre</sup>* allele that, like the wild-type allele (Frohman et al., 1990), is transiently expressed at low levels in the posterior hindbrain (Zhou et al., manuscript submitted for publication; data not shown).

### Second Branchial Arch Tissues in the Middle Ear Region of Wild-Type Embryos

The following presentation focuses on the distribution of labeled tissues in the otic region at embryonic day (E) 15.5, when the principal organization of the middle ear is established in the mouse (Mallo, 2001) (Fig. 2). The progression of second arch development was studied in a series of embryos ranging from E10.5 to E17.5. Labeled cells at all stages were clearly related to those present at preceding stages; novel, isolated populations of labeled cells that might suggest recombination of the marker after E10.5 were not observed.

At E15.5, the most-dorsal labeled

tissue was the connective tissue of the external ear (Fig. 2A,B). This area was continuous with labeled connective tissue surrounding the ventrolateral aspect of the pars canicularis of the otic capsule (Fig. 2B–D). Surprisingly, the cartilage that formed a portion of the ventrolateral aspect of the pars canicularis and the roof of the middle ear cavity (the tectum tympani) was also labeled. Anteriorly, this labeled cartilage was attached to the posterior process of the squamosal bone by labeled connective tissue (Fig. 2G). Ventrally, the labeled capsular cartilage was continuous with the base of the styloid process (see Fig. 4D).

Within the middle ear cavity, the labeled domain extended ventrally through connective tissue surrounding the facial nerve and into the head, crura, and base of the stapes (Figs. 2B,C, 3A). The superficial portion of the stapedia footplate and the annular ligament anchoring it to the oval window were not labeled (Noden, 1978), nor was the cartilage of the oval window and the rest of the pars cochlearis of the auditory capsule (Figs. 2B,C; 3A). The domain of labeled connective tissue extended ventrally from the stapes to surround the processus brevis of the malleus (Fig. 2D–F,H,I). The cartilage of the processus brevis itself expressed the lineage marker and its boundary with the unlabeled body of the malleus was sharply defined (Fig. 2H, also see Figs. 2D, 4G), even though there was no discontinuity in the distribution of cell nuclei that might indicate the presence of a physical boundary (Fig. 2I). The boundary in the malleus was similar to the sharp segregation of first and second arch cells observed at earlier stages (Fig. 1C). Within the processus brevis, small clusters of unlabeled cells were present (Fig. 2H,I). These clusters could have been unrecombined second arch cells or ectopic first arch cells. The first explanation appeared more likely, because labeled cells were extremely rare in other parts of the malleus (Fig. 2). Thus, any mixing that occurred would have to have been in one direction only to explain the absence of displaced labeled cells. Similar clusters of unlabeled cells were also observed within

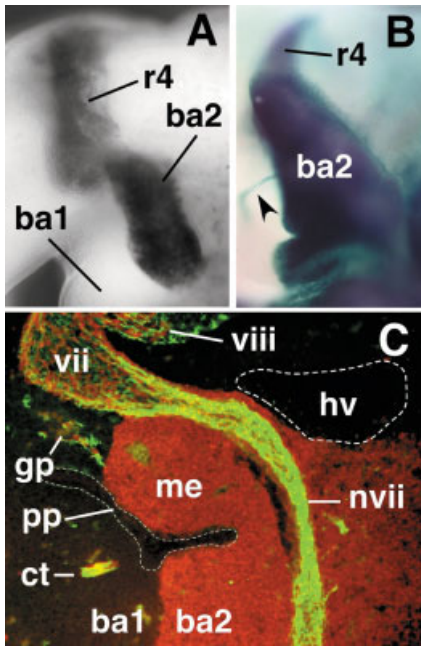


**Fig. 1.** Labeling of rhombomere 4 (r4) and second branchial arch mesenchyme in  $+ / B1^{Cre}$ ,  $+ / R26R$  embryos. **A:** Lateral view (anterior at left, dorsal at top) of an embryonic day (E) 9.5 embryo showing the histochemical labeling of r4 and the second branchial arch (ba2). The first branchial arch (ba1) is not labeled. **B:** An equivalent domain at E12.5, showing continued marker expression in ba2 and r4. The arrowhead points to the chorda tympani nerve. **C:** Sagittal section of an E12.5 embryo through the middle ear region (me) immunostained for the lineage marker (red) and  $\beta$ -tubulin (green) to label nerves. The labeled second arch domain is coherent and forms a sharp boundary with the first arch. Glial cells of facial nerve (nvii) branches, the chorda tympani (ct) and the greater petrosal (gp), are also labeled. hv, head vein; pp, pharyngeal pouch; vii and viii, facial and vestibuloacoustic ganglia.

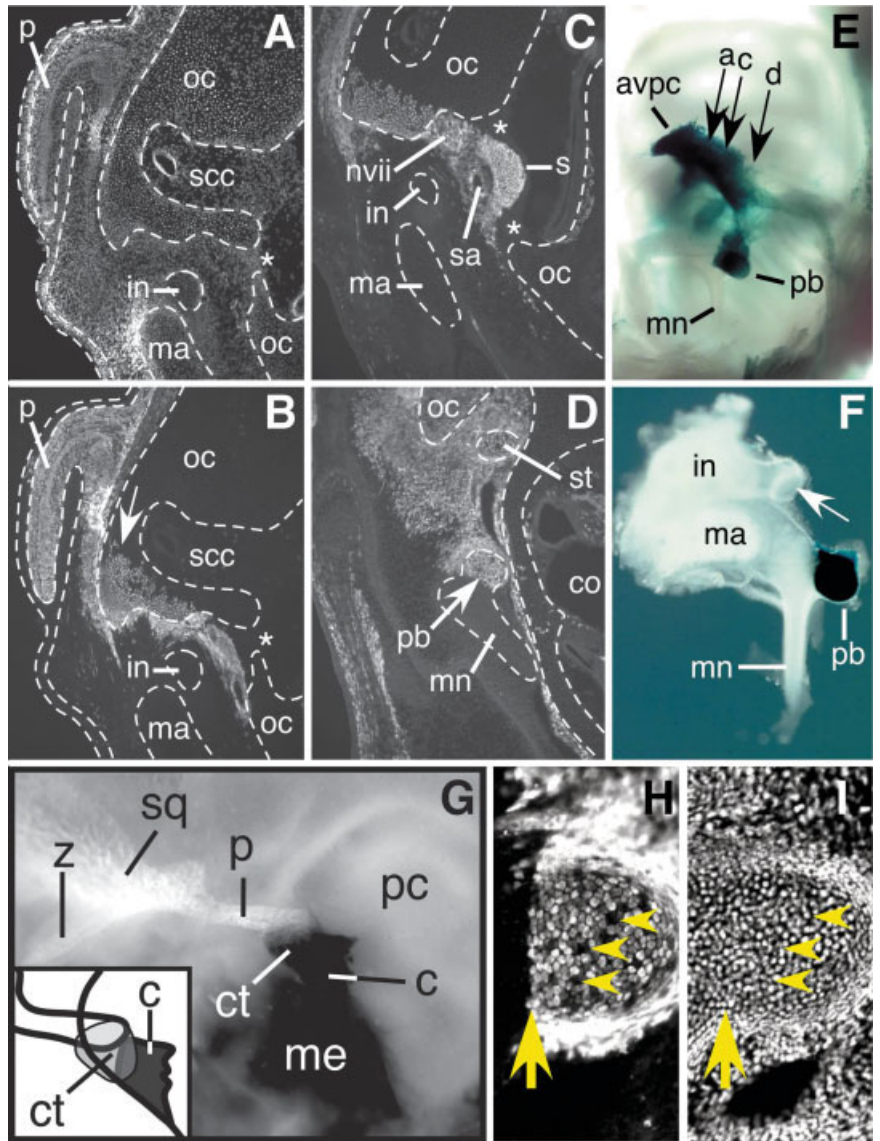


**Fig. 2.** Distribution of second arch tissues in the middle ear region. **A-D,H,I:** Immunolabeling of marker in sections of an embryonic day (E) 15.5 embryo. **E-G:** Histochemical demonstration of marker in dissected newborn specimens. Plane and level of sections shown in **A-D** are indicated (also see Fig. 3A). **A,B:** A transverse section through the anterior margin of the oval window (asterisks) showing 4',6-diamidino-2-phenylidole-dihydrochloride (DAPI) labeling of all cells (**A**) and marker activity in second arch cells (**B**), which appear white against the gray background. Marked cells formed connective tissue of the external ear (p) and surrounded the lateral aspect of the otic capsule (oc), formed the roof of the middle ear cavity (arrow in **B**), and connective tissue lateral to the oval window. **C:** More posteriorly, labeled tissue included the lateral margin of the otic capsule and connective tissue surrounding the facial nerve (nvii) and stapedia artery (sa). The stapes (s) was labeled, but the annular ligament (asterisks) binding it to the oval window was not (also see Fig. 3A). The incus (in) and the head of the malleus (ma) were unlabeled. **D:** More posterior section showing labeled cells in tissue surrounding the styloid process (st) and processus brevis (pb). Cartilage of the styloid process and processus brevis was labeled; the manubrium (mn) was not. **E:** Lateral view of the left otic capsule of a newborn mouse. Labeled tissue extended from the anteroventral margin of the pars canicularis of the otic capsule (avpc) through connective tissue into the processus brevis. **F:** Medial view of a right malleus and incus from a newborn pup. Only the processus brevis expressed the marker. Arrow indicates articular surface of crus longum. **G:** Lateral view of a newborn mouse skull showing the apposition of the posterior process (p) of the squamosal bone (sq) with labeled connective tissue (ct) and cartilage (c) of the pars canicularis (pc) of the otic capsule. The point of contact is diagrammed in the inset. **H,I:** The boundary (arrows) between unlabeled and labeled cells in the malleus is sharp; no physical boundary was seen in the DAPI staining of the same section (**I**). Small clusters of unlabeled cells were present within the labeled domain (arrowheads in **H,I**). co, cochlea; me, middle ear; scc, semicircular canal; z, zygomatic process.

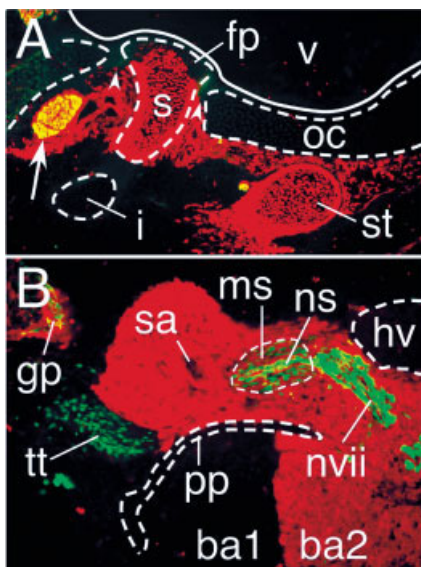


**Fig. 3.**

labeled domains of the stapes and otic capsule.

From the processus brevis, labeled connective tissue extended around the dorsal portion of the tympanic membrane and then ventrally along the medial wall of the auditory meatus (Fig. 2D). The connective tissue of the stapedius muscle and the Schwann cells of the stapedia nerve expressed the lineage marker, but the myocytes of the stapedius muscle itself and both the myocytes and connective tissue of the tensor tympani did not (Fig. 3B). These results are consistent with the hypothesis that the connective tissue of muscles innervated by the trigeminal and facial nerves is formed, respectively, by first and second arch crest (Kontges and Lumsden, 1996). Whether this explanation also holds for the facial mimetic musculature remains to be demonstrated.

### Second Branchial Arch Tissues in the Middle Ear Region of *Hoxa2* Mutant Embryos

The phenotype of *Hoxa2* null mutations includes the absence of external ears and the processus brevis, duplication of the malleus and the squamosal bone, and malformations of the otic capsule (Gendron-Maguire et al., 1993; Rijli et al., 1993). The present findings in wild-type embryos suggested that each of the supernumerary skeletal elements arises at sites where first and second arch skeletal el-

ements are normally apposed. This question was examined by combining a null mutation of *Hoxa2* (*Hoxa2*<sup>tm1Grid</sup> Gendron-Maguire et al., 1993) with the *B1<sup>Cre</sup>* and *R26R* alleles. The distribution of labeled cells at early stages (E9.5–E12.5) was not different in *Hoxa2* mutant embryos compared with embryos that were heterozygous or homozygous for the wild-type allele (data not shown). There was no evidence of ectopic *Hoxb1* or *Cre* expression in *Hoxa2* mutant embryos through E12.5 (data not shown).

At E15.5, duplications of the incus and malleus were apparent in *Hoxa2* mutant embryos (Fig. 4A,B). The axis of symmetry and the border between marked and unmarked cells was a roughly straight line along the posterior border of the orthotopic first arch elements. The axis of the malleal duplication was at the position where the processus brevis normally joins the malleus (Gendron-Maguire et al., 1993; Rijli et al., 1993) and extended through the manubrium (Fig. 4A–C). Labeled and unlabeled cell bodies were intermixed over distances of several cell diameters in the mallei of mutant embryos, to a greater degree than cells along the analogous border in wild-type embryos (compare Figs. 2H with 4C). As in wild-type embryos, clusters of unlabeled cells were present throughout the second arch-derived territory, but labeled cells were not found within the orthotopic first arch elements.

The axis of duplication for the incus occurred at the end of the orthotopic crus longum (Gendron-Maguire et al., 1993; Rijli et al., 1993). In wild-type embryos, the crus longum articulates with the stapes medially and abuts the styloid process posteriorly; both of these structures are derived from the second arch (Figs. 4F,G). In mutant embryos, labeled cartilage was not present in the otic capsule, but a labeled, rod-like cartilaginous element was present in the position of the styloid process (Fig. 4E). This element did not fuse with the otic capsule and may represent the duplicated tympanic bone described by others (Gendron-Maguire et al., 1993; Rijli et al., 1993). Similarly, the axis of symmetry for the squamosal duplication (Gendron-Maguire et al., 1993; Rijli et al., 1993) formed where the squamosal's

posterior process meets the second arch territory of the otic capsule (Fig. 2G, and data not shown). As noted above, second arch tissue did not contribute to the otic capsule of *Hoxa2* mutant embryos, suggesting that the mesenchymal domain that normally form the second arch capsular tissue of wild-type embryos could form the duplicated squamosal in mutant embryos.

## DISCUSSION

### Homologies and Evolutionary Considerations

Although the contribution of second arch neural crest cells to the external ear may be novel in mammals, the other skeletal derivatives described here (summarized in Fig. 5A) have parallels in other vertebrate classes. The fusion of first and second arch cartilages in the malleus is likely to reflect a process completed before the emergence of tetrapods. The malleus is homologous to the articular bone, a proximal element of the compound lower jaw of nonmammalian tetrapods (Romer and Parsons, 1977). The retroarticular process extends posteriorly from the articular and in birds is formed by metencephalic crest (Noden, 1983) that populates the second branchial arch (Kontges and Lumsden, 1996). The finding that the processus brevis arises from the second arch in mice argues that this mammalian element is homologous to the retroarticular process. It also weighs against the idea that the manubrium of the malleus is the homologue of the retroarticular process, as has often been proposed (Goodrich, 1958). The second arch derivation of the processus brevis also provides a cellular basis for the restricted phenotype observed in *Msx1* mutant embryos (Satokata and Maas, 1994), in which the processus brevis is missing but the rest of the malleus is spared.

Similarly, the incorporation of second arch tissues into the otic capsule is likely to predate the divergence of mammalian and avian lineages, for crest-derived capsular cartilage is present in birds also (Le Lievre, 1978; Noden, 1983; Couly et al., 1993), although it has not been established that the avian tissue arises from sec-

**Fig. 3.** Second arch lineages in the stapes. **A:** Section from a neonatal mouse showing the lineage marker (red) and neurofilament (green). The stapes (s), styloid process (st), and facial nerve (arrow) expressed the lineage marker. The surface of the stapedia footplate (fp) and the annular ligament (arrowheads) were not labeled. **B:** Sagittal section through the anlagen of an embryonic day (E) 13.5 stapes stained as in A but with the addition of an antibody to MyoD (green nuclear stain), which stains myoblasts. The stapedia artery (sa) was visible in the middle of the stapedia anlagen. The stapedius muscle (ms) myoblasts did not express the marker, they and the stapedia nerve (ns) were surrounded by cells that did. The tensor tympani (tt) did not contain labeled connective tissue. ba1 & ba2, first and second branchial arches; gp, greater petrosal nerve; hv, head vein; i, incus; oc, otic capsule; pp, pharyngeal pouch; nvii, facial nerve; v, vestibule of inner ear.

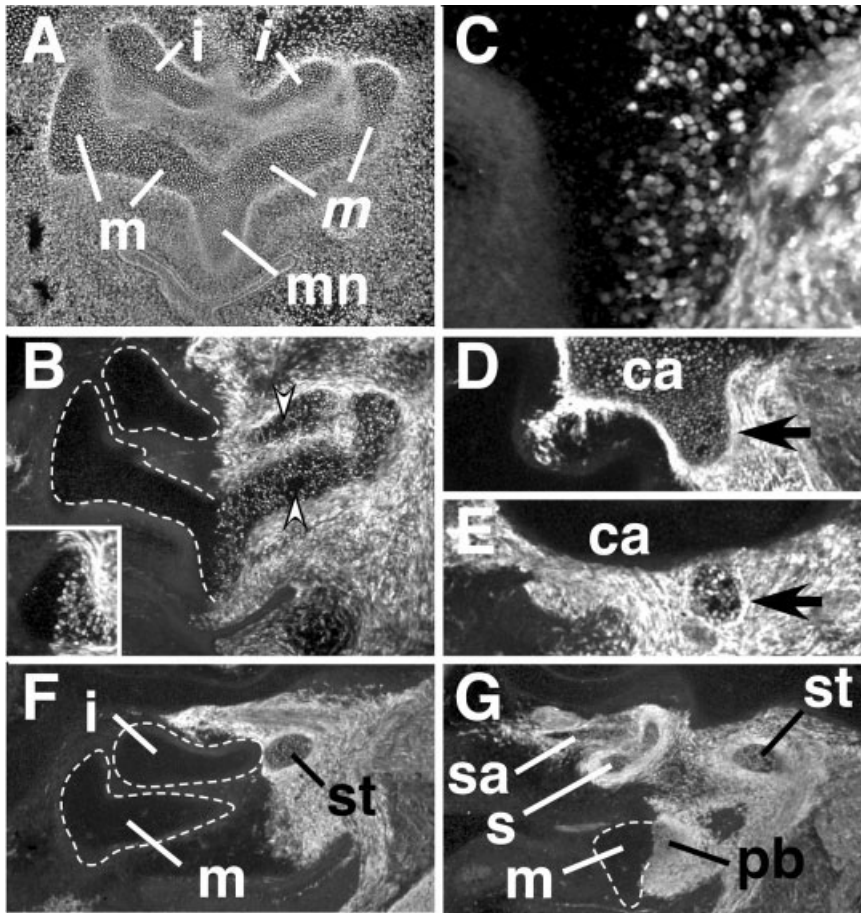


**Fig. 4.** Distribution of first and second arch tissue in sagittal sections of wild-type and *Hoxa2* mutant embryos. Anterior at left and dorsal at top, second arch cells appear white in B–G. **A,B:** The 4',6-diamidino-2-phenylidole-dihydrochloride (DAPI) staining (A) and marker expression (B) in an embryonic day (E) 15.5 *Hoxa2* mutant embryo. The boundary between unlabeled first arch and labeled second arch tissues runs between the orthotopic incus (i) and its duplication (i), and between the orthotopic malleus (m) and its duplication (m), and extends into the manubrium (mn). Arrowheads in B indicate unlabeled cells within the duplicated incus and malleus. Inset: Nearby section through the junction of the duplicated incus. **C:** Higher magnification of the malleus shown in A and B. The boundary between first and second arch domains is less sharply defined than in wild-type embryos (compare with Fig. 2H). **D,E:** Sections through the ventrolateral aspect of the pars canicularis (ca) of wild-type (D) and *Hoxa2* mutant (E) embryos at E15.5. Labeled second arch cartilage in the capsule of the wild-type embryo is continuous with the base of the styloid process (arrow, D), whereas in mutant embryos, the capsule is unlabeled and the second arch element (arrow, E) in the location of the styloid does not fuse with the capsule. **F:** The incus, malleus, and styloid process (st) of a wild-type embryo showing the crus longum of the incus close to the styloid process. **G:** More medial section shows that the curae of the stapes (s) are anterior to the styloid process and medial to the crus longum of the incus shown in F. sa, stapedial artery; pb, processus brevis.

ond arch crest. The second arch capsular domain described here appeared identical to a crest-derived domain illustrated by Noden in birds (Noden, 1983). This finding could result from the parallel evolution of a feature in two vertebrate classes, but more likely reflects the presence of second arch tissue in the capsule of a common precursor.

After Reichert (1837), discussions of the embryology and evolution of tetra-

pod second arch tissues have generally held that the stapes is the principal cartilage derived from the main dorsal (epihyal) element of the second arch, the hyomandibula, that formed a portion of the jaw suspension in tetrapod precursors. The other relatively dorsal second arch derivative widely recognized in the otic region of mammals is the styloid process, which has been considered variously to be homologous to a stylohyal, or laterohyal el-

ement intercalated between the ancestral hyomandibula and the principal ventral hyoid cartilage, the ceratohyal (Goodrich, 1958). The latter is generally thought to be represented in modern mammals by the stylohyoid ligament.

The results presented here could be interpreted in several ways relative to prevalent conceptions of second arch evolution. If stapelial elements are considered to be the only representation of the hyomandibula in modern forms, then the second arch capsular tissue must derive from another source. One possibility is the lateral commissure, an outcropping of the skull that forms the articular surface for the dorsal end of the hyomandibula in fishes and tetrapod precursors such as *Eusthenopteron*, and which some have considered homologous to the most dorsal (pharyngohyal) elements of the second arch (Jarvik, 1980). The fate of this element during the transition to tetrapods is poorly understood (Clack, 2002), and it is possible that it is retained as the capsular tissue described here. Alternatively, the second arch capsular tissue could represent a neomorphic expansion of laterohyal or stylohyal elements homologous to the styloid process.

Alternatively, given that prevalent conceptions of second arch evolution were formulated without knowledge of the second arch tissue in the otic capsule, it is reasonable to consider that more of the ancestral hyomandibula is preserved in modern tetrapods than previously thought. Earlier hyomandibular homologues, such as the stapes of early synapsids (e.g., pelycosaurs), were substantial elements, often with two proximal heads (Bolt and Lombard, 1992) (Fig. 5B). The more medial and ventral head contacted the oval window and contained the stapedial canal, while the more lateral and dorsal head attached to the otic region of the skull. It has been suggested that the dorsal process of the stapes was much reduced in later tetrapods, that relatively minor derivatives are found in the tympanohyal of modern forms, and that much of the body of the stapes disappeared (Allin and Hopson, 1992). An alternative progression suggested by the present results is that the ventral head of the ancestral stapes became isolated from

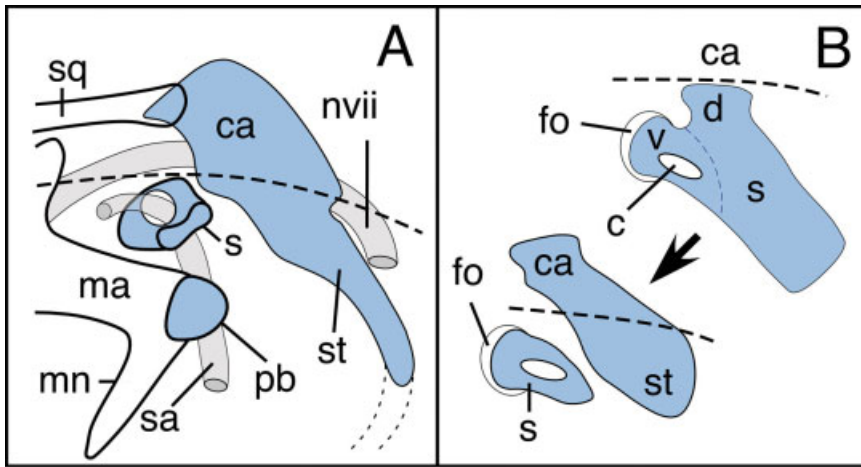


**Fig. 5.** A,B: Summary of second arch lineages in wild-type mice (A) and a model of stapes evolution (B). **A:** The second arch cartilages are shaded dark grey, and the facial nerve (nvii) and stapedia artery (sa) are shaded light gray. The incus and second arch connective tissues are not shown for clarity. The dashed line indicates the position of the ventrolateral margin of the pars canicularis; the malleus (ma), stapes (s), and facial nerve (nvii) are medial to this. **B:** The stapes of a pelycosaur is shown in the upper right portion of the diagram (Allin and Hopson, 1992; Bolt and Lombard, 1992), with the ventral (v) proximal head apposed to the oval window (fo) and pierced by the stapedia canal (c), and the dorsal head (d) contacting the otic capsule (ca). At lower left is the proposed separation of the ventral head (e.g., along dashed line shown above) as the stapes of later forms, and fusion of the dorsal head and body with the otic region as capsular cartilage (ca) and the styloid process (st). mn, manubrium; pb, processus brevis; sq, posterior process of squamosal.

the rest at a relatively early stage and formed the stapes of modern tetrapods (Fig. 5B). In parallel, the dorsal head and most of the body of the stapes fused with the otic capsule as second arch capsular tissue and the base of the styloid process. The original relationship between the two derivatives of the ancestral stapes is preserved in that the modern stapes is medial and ventral to the second arch capsular tissue to which it is connected by a band of second arch connective (Figs. 2C, 5A).

Whereas this model is most easily reconciled with an ancestral stapes with two proximal heads, of which the more ventral inserted into the oval window, it is consistent with alternative ancestral forms also. A minor corollary is that the boundary between epihyal and stylo- or laterohyal elements, poorly known from paleontological data, would be placed at a more ventral position than is generally thought, near the distal extreme of the styloid process or within the dorsal portion of the stylohyal ligament.

### **Hoxa2 Mutant Phenotype**

Second arch cartilages that could be transformed into the duplicated squa-

mosal and malleus of *Hoxa2* mutant embryos had not been identified previously. It has been unclear, therefore, whether the duplicated elements were formed by tissues that normally expressed a potential to form cartilage. Here, each duplication was found to form at a site where first and second arch skeletal elements were either fused or closely apposed in wild-type embryos. The duplicated malleus formed at the site where the missing processus brevis is normally fused to the body of the malleus. The duplicated squamosal formed at the point where the squamosal bone is normally apposed to second arch cartilage of the otic capsule, and the latter is missing in mutant embryos. As previously recognized, the duplicated incus is formed at the site where the incus normally meets the second arch stapes. The present data do not establish that the same second arch cells are recruited to form skeletal elements in both wild-type and mutant embryos; but they nonetheless clearly establish that the duplicated skeletal elements of *Hoxa2* mutant embryos form within domains of second arch mesenchyme from which cells are normally recruited to form skeletal elements.

This alignment of first and second arch skeletal elements along the proximodistal axis of the first two branchial arches in both wild-type and *Hoxa2* mutant embryos argues that the mechanisms that initiate cartilage and bone formation act in a similar manner on both arches. Such a mechanism has been invoked previously to explain the symmetrical arrangement of duplicated elements in the mutants (Rijli et al., 1993). The relationship between potentially inductive mechanisms, which could include interactions with pharyngeal tissues (Epplein, 1978; Piotrowski and Nusslein-Volhard, 2000; Couly et al., 2002; Crump et al., 2004) or the activities of genes expressed in one or both of the first two arches themselves (Satokata and Maas, 1994; Martin et al., 1995; Rivera-Perez et al., 1995; Qiu et al., 1997; Yamada et al., 1997; Clouthier et al., 1998; Depew et al., 2002), with *Hoxa2* function is likely to be complex. It has been suggested that *Hoxa2* function in the second arch domain renders some cells incapable of responding to these signals and causes a dorsal shift of the spatial domains that can respond (Kanzler et al., 1998). At the time chondrogenesis begins in the anlagen of the stapes and styloid process, the chondrogenic condensations do not express *Hoxa2*, which continues to be expressed in immediately surrounding mesenchyme. This and the complementary relationship between *Hoxa2* and *Sox9* expression provides strong evidence that *Hoxa2* function inhibits chondrogenesis (Kanzler et al., 1998) in what may be a context-dependent manner (Creuzet et al., 2002).

*Hoxa2* appears to be expressed by virtually all second arch crest at early stages of branchial arch morphogenesis (Prince and Lumsden, 1994; Couly et al., 1998). The absence of *Hoxa2* expression in the anlagen of the stapes and styloid process, therefore, is more likely to represent a focal down-regulation of expression than a sorting of nonexpressing second arch cells into specific chondrogenic domains. In this light, the results presented here suggest a model in which *Hoxa2* expression is locally inhibited by the mechanisms that determine the common dorsoventral positions of first and second arch skeletal elements and

that the continued *Hoxa2* expression in the surrounding mesenchyme limits the extent of skeletogenesis to generate the second arch elements observed in wild-type embryos.

The absence of second arch tissue in the otic capsule of *Hoxa2* null embryos suggests that *Hoxa2* function may be required for the normal integration of second arch crest cells into the capsule. If, as proposed above, these instead form the duplicated squamosal, then they also switch from an endochondral to an intramembranous pathway of bone formation. This conversion is likely to be secondary to the failure of second arch cells to fuse with other capsular tissues, for the surrounding cellular milieu is known to strongly influence the osteogenic pathways followed by neural crest cells (McGonnell and Graham, 2002; Abzhanov and Tabin, 2004).

Although *Hoxa2* function controls many aspects of the differentiation of second arch tissues, it does not significantly influence the migration of second arch neural crest cells or the overall segregation of first and second arch crest. In both wild-type and mutant embryos, the boundary between first and second arch cells was at the posterior ends of normally positioned first arch elements. At a finer level, there was more mixing of labeled and unlabeled cells about the border between first and second arch domains in the malleus. This finding, and the failure of second arch crest cells to integrate into the otic capsule, suggest that *Hoxa2* function, among other potential activities, is required for the normal expression of cell surface adhesion or signaling molecules that influence local interactions of second arch neural crest cells and their neighbors.

## EXPERIMENTAL PROCEDURES

### Mice

The preparation of the *Hoxb1-Cre* allele (*B1<sup>Cre</sup>*) has been described elsewhere (Zhou et al., manuscript submitted for publication). Briefly, a targeting construct was prepared in which a Cre recombinase coding sequence was fused in frame with the *Hoxb1* coding sequence shortly after

the translation initiation codon. The vector was transfected into embryonic stem cells and recombinant clones were used to generate lines of mice. Mice homozygous for the recombinant allele had phenotypes identical to reported null alleles of *Hoxb1* (Goddard et al., 1996; Studer et al., 1996). Mice with a null allele of *Hoxa2* (*Hoxa2<sup>tm1Grid</sup>*; Gendron-Maguire et al., 1993) were obtained from Jackson Laboratories. Mice bearing the Cre-conditional *R26R* reporter allele (Soriano, 1999) were obtained from Philippe Soriano. Each strain was maintained by backcrossing to B6D2F1 hybrids; variations in the phenotypes of the alleles were not observed during backcrossing. For timed pregnancies, noon of the day a copulation plug was found was designated E0.5.

### Immunohistochemistry

Embryos were harvested in phosphate buffered saline (PBS) and fixed in 4% phosphate-buffered formaldehyde for 1–4 hr, washed in PBS, and equilibrated with 30% sucrose for frozen sectioning. Sections were blocked with 5% normal donkey serum in PBST (PBS plus 0.3% Triton) and primary antibodies were applied overnight at 4°C. Primary antibodies included goat (Biogenesis, 1:3,000) and rabbit (Cappel, 1:5,000) anti- $\beta$ -galactosidase, mouse anti- $\beta$ -tubulin (Tuj1) (Babco, 1:1,000; Lee et al., 1990), and rabbit anti-neurofilament (Sigma, 1:3,000). Secondary antibodies (Jackson Immunochemicals) conjugated to either Cy3 or fluorescein isothiocyanate were applied for 2 hr. Histological material was examined and photographed with a Zeiss Axioskop microscope equipped with a Hamamatsu digital camera and Openlab software (Improvision).

### ACKNOWLEDGMENTS

The author thanks Edgar F. Allin and Jennifer A. Clack for extremely helpful correspondence about the manuscript, Allison Hall for helpful discussions, and Yuefang Zhou, Erin Barcarse, Chung-Wen Liu, Katherine Lobur, Amy Lucky, Min Qian, and Tam Trieu for assistance at various stages of this study.

## REFERENCES

- Abzhanov A, Tabin CJ. 2004. Shh and Fgf8 act synergistically to drive cartilage outgrowth during cranial development. *Dev Biol* 273:134–148.
- Allin EF. 1975. Evolution of the mammalian middle ear. *J Morphol* 147:403–437.
- Allin EF, Hopson JA. 1992. Evolution of the auditory system in synapsida (“mammal-like reptiles” and primitive mammals) as seen in the fossil record. In: Webster DB, Fay RR, Popper AN, editors. *The evolutionary biology of hearing*. New York: Springer-Verlag. p 587–614.
- Bolt JR, Lombard RE. 1992. Nature and quality of fossil evidence for otic evolution in early tetrapods. In: Webster DB, Fay RR, Popper AN, editors. *The evolutionary biology of hearing*. New York: Springer-Verlag. p 377–403.
- Clack JA. 2002. Gaining ground. The origin and evolution of tetrapods. Bloomington, IN: Indiana University Press. 369 p.
- Clouthier DE, Hosoda K, Richardson JA, Williams SC, Yanagisawa H, Kuwaki T, Kumada M, Hammer RE, Yanagisawa M. 1998. Cranial and cardiac neural crest defects in endothelin-A receptor-deficient mice. *Development* 125:813–824.
- Couly G, Creuzet S, Bennaceur S, Vincent C, Le Douarin NM. 2002. Interactions between Hox-negative cephalic neural crest cells and the foregut endoderm in patterning the facial skeleton in the vertebrate head. *Development* 129:1061–1073.
- Couly G, Grapin BA, Coltey P, Ruhin B, Le Douarin NM. 1998. Determination of the identity of the derivatives of the cephalic neural crest: incompatibility between Hox gene expression and lower jaw development. *Development* 125:3445–3459.
- Couly GF, Coltey PM, Le Douarin NM. 1993. The triple origin of skull in higher vertebrates: a study in quail-chick chimeras. *Development* 117:409–429.
- Creuzet S, Couly G, Vincent C, Le Douarin NM. 2002. Negative effect of Hox gene expression on the development of the neural crest-derived facial skeleton. *Development* 129:4301–4313.
- Crump JG, Swartz ME, Kimmel CB. 2004. An integrin-dependent role of pouch endoderm in hyoid cartilage development. *PLoS Biol* 2:E244.
- Depew MJ, Lufkin T, Rubenstein JL. 2002. Specification of jaw subdivisions by *Dlx* genes. *Science* 298:381–385.
- Epperlein HH. 1978. The ectomesenchymal-endodermal interaction system of *Triturus alpestris* in tissue culture: morphological and histochemical characterization of developing neural derivatives. *Differentiation* 11:109–123.
- Frohman MA, Boyle M, Martin GR. 1990. Isolation of the mouse *Hox-2.9* gene; analysis of embryonic expression suggests that positional information along the anterior-posterior axis is specified by mesoderm. *Development* 110:589–607.

- Gendron-Maguire M, Mallo M, Zhang M, Gridley T. 1993. *Hoxa-2* mutant mice exhibit homeotic transformation of skeletal elements derived from cranial neural crest. *Cell* 75:1317–1331.
- Goddard JM, Rossel M, Manley NR, Capocchi MR. 1996. Mice with targeted disruption of *Hoxb-1* fail to form the motor nucleus of the VIIIth nerve. *Development* 122:3217–3228.
- Goodrich ES. 1958. *Studies on the structure and development of vertebrates*. New York: Dover Publications. 485 p.
- Grammatopoulos GA, Bell E, Toole L, Lumsden A, Tucker AS. 2000. Homeotic transformation of branchial arch identity after *Hoxa2* overexpression. *Development* 127:5355–5365.
- Jarvik E. 1980. *Basic structure and evolution of vertebrates*. Vol. 2. New York: Academic Press. 237 p.
- Kanzler B, Kuschert SJ, Liu YH, Mallo M. 1998. *Hoxa-2* restricts the chondrogenic domain and inhibits bone formation during development of the branchial area. *Development* 125:2587–2597.
- Kontges G, Lumsden A. 1996. Rhombencephalic neural crest segmentation is preserved throughout craniofacial ontogeny. *Development* 122:3229–3242.
- Le Douarin N. 1983. *The neural crest*. Cambridge: Cambridge University Press.
- Le Lievre CS. 1978. Participation of neural crest-derived cells in the genesis of the skull in birds. *J Embryol Exp Morphol* 47:17–37.
- Lee MK, Tuttle JB, Rebhun LI, Cleveland DW, Frankfurter A. 1990. The expression and posttranslational modification of a neuron-specific beta-tubulin isotype during chick embryogenesis. *Cell Motil Cytoskeleton* 17:118–132.
- Lumsden A, Sprawson N, Graham A. 1991. Segmental origin and migration of neural crest cells in the hindbrain region of the chick embryo. *Development* 113:1281–1291.
- Mallo M. 2001. Formation of the middle ear: recent progress on the developmental and molecular mechanisms. *Dev Biol* 231:410–419.
- Martin JF, Bradley A, Olson EN. 1995. The paired-like homeo box gene *MHox* is required for early events of skeletogenesis in multiple lineages. *Genes Dev* 9:1237–1249.
- McGonnell IM, Graham A. 2002. Trunk neural crest has skeletogenic potential. *Curr Biol* 12:767–771.
- Noden DM. 1978. The control of avian cephalic neural crest cytodifferentiation. I. Skeletal and connective tissues. *Dev Biol* 67:296–312.
- Noden DM. 1983. The role of the neural crest in patterning of avian cranial skeletal, connective, and muscle tissues. *Dev Biol* 96:144–165.
- O’Gorman S, Fox DT, Wahl GM. 1991. Recombinase-mediated gene activation and site-specific integration in mammalian cells. *Science* 251:1351–1355.
- Piotrowski T, Nusslein-Volhard C. 2000. The endoderm plays an important role in patterning the segmented pharyngeal region in zebrafish (*Danio rerio*). *Dev Biol* 225:339–356.
- Prince V, Lumsden A. 1994. *Hoxa-2* expression in normal and transposed rhombomeres: independent regulation in the neural tube and neural crest. *Development* 120:911–923.
- Qiu M, Bulfone A, Ghattas I, Meneses JJ, Christensen L, Sharpe PT, Presley R, Pedersen RA, Rubenstein JL. 1997. Role of the *Dlx* homeobox genes in proximodistal patterning of the branchial arches: mutations of *Dlx-1*, *Dlx-2*, and *Dlx-1* and *-2* alter morphogenesis of proximal skeletal and soft tissue structures derived from the first and second arches. *Dev Biol* 185:165–184.
- Reichert C. 1837. *Über die Visceralbogen der Wirbeltiere im allgemeinen und deren Metamorphosen bei den Vögeln und Saugetieren*. *Arch Anat Physiol* 1837:120–222.
- Rijli FM, Mark M, Lakkaraju S, Dierich A, Dolle P, Chambon P. 1993. A homeotic transformation is generated in the rostral branchial region of the head by disruption of *Hoxa-2*, which acts as a selector gene. *Cell* 75:1333–1349.
- Rivera-Perez JA, Mallo M, Gendron-Maguire M, Gridley T, Behringer RR. 1995. Goosecoid is not an essential component of the mouse gastrula organizer but is required for craniofacial and rib development. *Development* 121:3005–3012.
- Romer AS, Parsons TS. 1977. *The vertebrate body*. Philadelphia: Saunders. 624 p.
- Satokata I, Maas R. 1994. *Msx1* deficient mice exhibit cleft palate and abnormalities of craniofacial and tooth development. *Nat Genet* 6:348–356.
- Serbedzija GN, Bronner-Fraser M, Fraser SE. 1992. Vital dye analysis of cranial neural crest cell migration in the mouse embryo. *Development* 116:297–307.
- Soriano P. 1999. Generalized *lacZ* expression with the ROSA26 Cre reporter strain. *Nat Genet* 21:70–71.
- Strickland EM, Anson BJ. 1962. Branchial sources of auditory ossicles in man. I. Literature. *Arch Otolaryngol* 76:100–122.
- Studer M, Lumsden A, Ariza ML, Bradley A, Krumlauf R. 1996. Altered segmental identity and abnormal migration of motor neurons in mice lacking *Hoxb-1*. *Nature* 384:630–634.
- Yamada G, Ueno K, Nakamura S, Hanamura Y, Yasui K, Uemura M, Eizuru Y, Mansouri A, Blum M, Sugimura K. 1997. Nasal and pharyngeal abnormalities caused by the mouse goosecoid gene mutation. *Biochem Biophys Res Commun* 233:161–165.
- Zhou YA, Barcarse EA, O’Gorman S. Submitted. Altered neuronal lineages in the facial ganglia of *Hoxa2* mutant mice.